Earth Mineral dust source InvesTigation (EMIT)

EMIT L2b Algorithm: Mineral Detection and Related Products at the Pixel Scale

Theoretical Basis

Roger N. Clark, Planetary Science Institute, Tucson AZ
Gregg A. Swayze, U. S. Geological Survey, Denver, CO
Vincent J. Realmuto, Jet Propulsion Laboratory, Pasadena, CA
Philip G. Brodrick, Jet Propulsion Laboratory, Pasadena, CA
David R. Thompson, Jet Propulsion Laboratory, Pasadena, CA

Version 0.2

April 2020

Jet Propulsion Laboratory
California Institute of Technology
Pasadena, California 91109-8099

Change Log

Version	Date	Comments
0.1	Sept, 2019	Initial Draft
0.2	March 2020	Refinement for demo SDS

Table of Contents

1. Key Teammebers

A large number of individuals contributed to the development of the algorithms, methods, and implementation of the L3 approach for EMIT. The primary contributors are the following:

- Roger N. Clark (Planetary Science Institute)
- Gregg A. Swayze (U.S. Geological Survey)
- Vincent J. Realmuto (Jet Propulsion Laboratory)
- Philip G. Brodrick (Jet Propulsion Laboratory)
- David R. Thompson (Jet Propulsion Laboratory)

2. Historical Context and Background on the EMIT Mission and its Instrumentation

Mineral dust aerosols originate as soil particles lifted into the atmosphere by wind erosion. Mineral dust created by human activity makes a large contribution to the uncertainty of direct radiative forcing (RF) by anthropogenic aerosols (USGCRP and IPCC). Mineral dust is a prominent aerosol constituent around the globe. However, we have poor understanding of its direct radiative effect, partly due to uncertainties in the dust mineral composition. Dust radiative forcing is highly dependent on its mineral-specific absorption properties. The current range of iron oxide abundance in dust source models translates into a large range of values, even changing the sign of the forcing (-0.15 to 0.21 W/m2) predicted by Earth System Models (ESMs) (Li et al., 2020). The National Aeronautics and Space Administration (NASA) recently selected the Earth Mineral Dust Source Investigation (EMIT) to close this knowledge gap. EMIT will launch an instrument to the International Space Station (ISS) to directly measure and map the soil mineral composition of critical dust-forming regions worldwide.

The EMIT Mission will use imaging spectroscopy across the visible shortwave (VSWIR) range to reveal distinctive mineral signatures, enabling rigorous mineral detection, quantification, and mapping. The overall investigation aims to achieve two objectives:

1. Constrain the sign and magnitude of dust-related RF at regional and global scales. EMIT achieves this objective by acquiring, validating and delivering updates of surface mineralogy used to initialize ESMs,
2. Predict the increase or decrease of available dust sources under future climate scenarios. EMIT achieves this objective by initializing ESM forecast models with the mineralogy of soils exposed within at-risk lands bordering arid dust source regions.

The EMIT instrument is a Dyson imaging spectrometer that will resolve the distinct spectral absorptions of iron oxides, clays, sulfates, carbonates, and other dust-forming minerals with contiguous spectroscopic measurements in the visible to short wavelength infrared region of the spectrum. EMIT will map mineralogy with a spatial sampling to detect minerals at the one hectare scale and coarser, ensuring accurate characterization of the mineralogy at the grid scale required by ESMs. EMIT's fine spatial sampling will resolve the soil exposed within hectare-scale agricultural plots and open lands of bordering arid regions, critical to understanding feedbacks caused by mineral dust arising from future changes in land use, land cover, precipitation, and regional climate forcing.

The EMIT Project is part of the Earth Venture-Instrument (EV-I) Program directed by the Program Director of the NASA Earth Science Division (ESD). EMIT is comprised of a VSWIR Infrared Dyson imaging spectrometer adapted for installation on the International Space Station (ISS).

Table 1 below describes the different data products the EMIT Mission will provide to the data archives. This document describes the "Level 2b" stage which relies on outputs from the Level 2A algorithms (cloud masking, standing water, vegetation cover) and the Level 2B mineral detection algorithms to produce mineral maps that can be aggregated (L3) and assimilated into Earth System models to evaluate Radiative Forcing (RF) impacts (Level 4).

Table 1. Emit Data Product Hierarchy

Data Product	Description	Initial Availability	Median Latency Post-delivery	NASA DAAC
Level 0	Raw collected telemetry.	4 months after IOC	2 months	LP DAAC
Level 1a	Reconstructed, depacketized, uncompressed data, time referenced, annotated with ancillary information reassembled into scenes.	4 months after IOC	2 months	LP DAAC
Level 1b	Level 1a data processed to sensor units including geolocation and observation geometry information.	4 months after IOC	2 months	LP DAAC
Level 2a	Surface reflectance derived by screening clouds and correction for atmospheric effects.	8 months after IOC	2 months	LP DAAC
Level 2b	Mineralogy derived from fitting reflectance spectra, screening for non-mineralogical components.	8 months after IOC	2 months	LP DAAC
Level 3	Gridded map of mineral composition aggregated from Level 2b with uncertainties and quality flags.	11 months after IOC	2 months	LP DAAC
Level 4	Earth System Model runs to address science objectives	16 months after IOC	2 months	LP DAAC

The Level 2b step can be loosely summarized through Error! Reference source not found., whereby measured reflectance as reported by Level 2a is used in combination with a spectral library and a series of mineral detection algorithms to produce mineral distribution maps. Significant additional details are discussed in Section 4. A high-level, yet complete, workflow of the EMIT science data system is shown in Figure 1 for context.

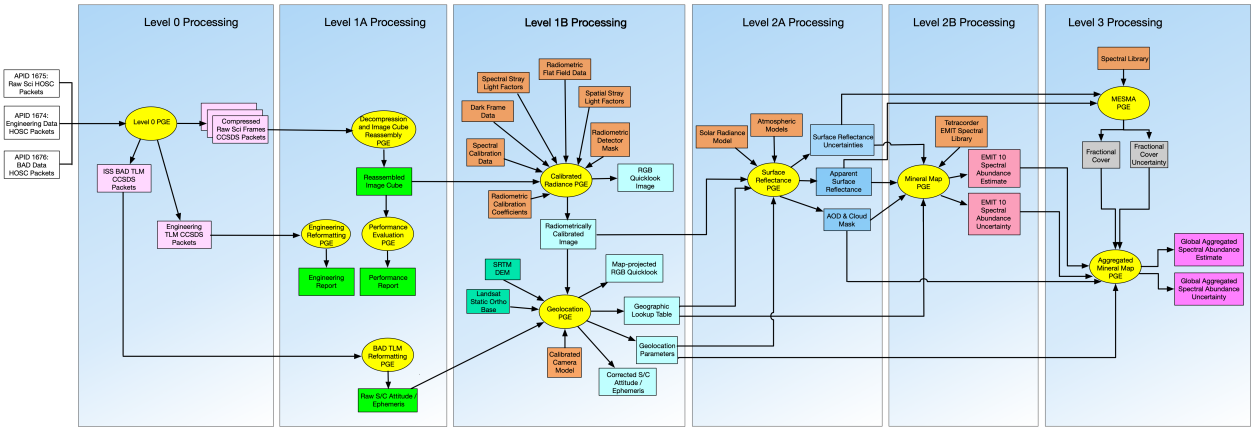

Figure 1. High-level workflow of the EMIT science data system.

3. Algorithm Rationale

The EMIT L2b approach builds on a substantial history of mineral identification with airborne imaging spectrometers. We leverage the Tetracorder system (Clark et al., 2003), which has been developed for over 30 years by spectroscopists at the U.S. Geological Survey and the Planetary Science Institute, along with additional collaborators. The Tetracorder mineral identification approach has been validated at numerous desert sites throughout the Southwestern U.S. (Clark et al., 2003; Swayze 1997; Swayze et al., 2014) using the Airborne Visible Infrared Imaging Spectrometer (AVIRIS-C, Green et al., 1998). Tetracorder has also been shown to be effective in a wide variety of environmental investigations (e.g. Swayze et al., 2000, 2009, 2014; Clark et al., 2001, 2006; Livo et al., 2007), demonstrating the general applicability of the approach.

4. Algorithm Description

4.1 Input data

The EMIT input and output data products delivered to the DAAC use their formatting conventions, the system operates internally on data products stored as binary data cubes with detached human-readable ASCII header files. The precise formatting convention adheres to the ENVI standard, accessible (Jan 2020) at https://www.harrisgeospatial.com/docs/ENVIHeaderFiles.html. The header files all consist of data fields in equals-sign-separated pairs, and describe the layout of the file. In the file descriptions below, *n* denotes the number of lines particular to the given acquisition.

The specific input files needed for the L2b stage are:

1. **Surface reflectance,** provided as an *n* x 1280 x *c* BIL interleave data cube, where each of *c* channels corresponds to a different wavelength.
2. **Channelized surface reflectance uncertainty,** provided as an *n* x 1280 x *c* BIL interleave data cube, where each of *c* channels corresponds to a different wavelength.

4.2 Theoretical description

The goal of the Level 2b step is to quantify surface minerology based on surface reflectance. Surface mineral detection relies on the distinct spectral signatures over the 400-2500 nm spectral region, as demonstrated for the EMIT-10 minerals in Figure 2. Mapping these minerals requires

in situ knowledge of the spectral reflectance of minerals as well as a system to match that *in situ* knowledge to remotely-sensed surface reflectance in a manner that minimizes the risk of misidentification.

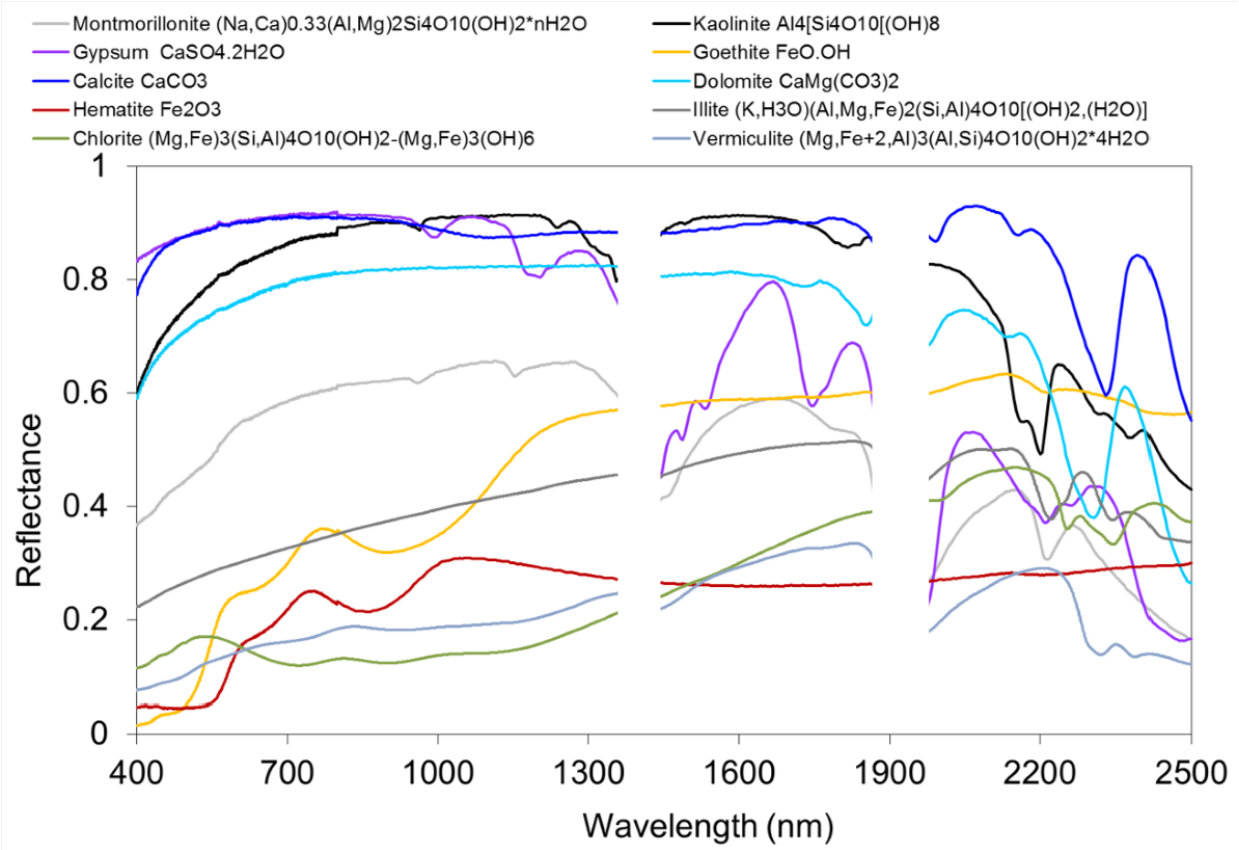

Figure 2. Reflectance spectra in the VSWIR spectral region for the designated EMIT dust source minerals. These spectra demonstrate distinct spectral signatures in specific regions, which facilitates mapping mineral composition.

Level 2b outputs are essentially generated in two steps. First, the strength of the spectral signature of a wide range of surface constituents is determined by feature matching L2a surface reflectance with spectra of reference minerals selected from the USGS Spectral Library 06 (Clark et al. 2007) using the Tetracorder system (Clark et al., 2003; see Section 4.2.1). Next, the strengths of the spectral signatures of key reference constituents are aggregated to estimate the spectral abundance of each of the EMIT 10 minerals (Section 4.2.2). Two additional spectral abundances are estimated as well, one containing "all additional iron oxides," and another containing "all other minerals."

4.2.1 Surface constituent mapping

Surface material mapping is performed following the procedure of the Tetracorder system, and ultimately generates independent maps for each reference library constituent Surface materials include not only pure components, but also mixtures of components (e.g., multiple minerals in areal, intimate, and molecular mixtures, coatings,, minerals and plant combinations, etc.). While the spectral identification process is documented in detail in Clark et al. (2003), in brief, it occurs by matching absorption features of predefined spectral regions to selected spectra from a reference library convolved to the EMIT spectrometer's spectral resolution. Spectral features for

the EMIT mission will come from the Tetracorder 5.2 command file cmd.lib.setup.t5.2b2. For each pixel *i*, all remotely sensed spectra are continuum-normalized for each spectral feature as

$$O_j^i(w) = 1 - \frac{R(w)}{C(w)}, \tag{1}$$

where R is the observed apparent surface reflectance input from L2a, C is the continuum reflectance linearly interpolated between two preselected continuum endpoints of the spectral feature of interest, and O is the continuum-normalized observed spectra. O, C, and R functions of wavelength (w). Corresponding continuum-normalized values for the library reference materials, L_j, are also calculated. As described in Clark et al. (2003), on a per-pixel basis, L_j is scaled by a constant linear factor a_j^i and offset by a second linear factor b_j^i to best match O_j^i over the full spectral feature, as

$$a_j^i = \text{argmin} \sum_{w \in W} \left(\left(a_j^i \, L_j^i(w) + b_j^i \right) - O_j^i(w) \right)^2 \tag{2}$$

$$= \frac{n \sum_{w \in W} O_j^i(w) L_j(w) - \sum_{w \in W} O_j^i(w) \sum_{w \in W} L_j(w)}{n \sum_{w \in W} L_j^2(w) - \left(\sum_{w \in W} L_j(w) \right)^2} \tag{3}$$

where W is the wavelength range of the given features, and a and b are linear coefficients. The quality of the feature match between continuum-removed (and scaled) spectra for constituent j is then calculated as the correlation coefficient F, adapted from Clark et al. (2003) as:

$$F_j = \frac{n \sum_{w \in W} O_j^i(w) L_j(w) - \sum_{w \in W} O_j^i(w) \sum_{w \in W} L_j(w)}{n \sum_{w \in W} \left(L_j^2(w) + O_j^{i\,2}(w) \right) - \left(\sum_{w \in W} L_j(w) \right)^2 + \left(\sum_{w \in W} O_j(w) \right)^2} \tag{4}$$

when all sums are calculated over the wavelength interval W for the given spectral feature which has n channels.

This fit is calculated for all selected reference spectra within a designated spectral region (i.e., a spectral group). The reference spectrum with the best fit is identified as the "observed" material within the given spectral region for the particular EMIT observed spectra. Spectral matches have to meet predetermined requirements, placed on factors such as goodness of fit, depth, the product of depth and fit, reflectance level (brightness), continuum slope, and/or the presence/absence of key ancillary spectral features. Spectral matches that fail to meet these requirements are discarded. Requirements are established in the Tetracorder 5.15 command file cmd.lib.setup.t5.2b2. The linear factor a_j^i provides a measure of how well the observed spectrum matches the reference spectrum j, and is assumed to be proportional to the surface area of the ground covered by constituent j.

The derived band depth for a spectral feature is proportional to the abundance of the material in the pixel. For areal mixtures this is a linear relationship but for intimate mixtures and coatings, it can be a nonlinear. However, nonlinearity depends on the reflectance change between the continuum and band center, and as a function of grain size. Tetracorder mitigates the grain size problem by deriving grain size when the factor is strong enough to show spectral differences. Then the relative abundance of the mineral signature in a pixel in the optical surface is assumed

to be proportional to the band strength relative to the reference spectra band strength and the abundance of the mineral in the reference spectrum. This relation is strictly true for areal mixtures and close to linear for the typical terrestrial arid soils EMIT will measure. The derived abundance is assumed to be uniform over a pixel for intimate mixtures, and fractional area for areal mixtures, but results in the same abundance value regardless of mixture type when carried forward for L3 aggregation.

The spectral features defined in the Tetracorder command file cmd.lib.setup.t5.2b2 include 23 spectral groups in total, which are reduced to those that are spanned by the wavelengths measured by EMIT, and are shown in Table 2. The dominant mineral detection groups, Groups 1 and 2, are basically the same as in Clark et al. (2003, 2010) and Swayze et al. (2003, 2014), with minor improvements made by subsequent studies.

Table 2. Tetracorder EMIT Expert System Groups and Cases

Group	Function
Group 0	Catchall for materials common to all other spectral groups
Group 1	Electronic absorptions in the visible and 1-micron regions
Group 2	Narrow absorptions in the 2 to 2.5-micron region (e.g. clays, carbonates, sulfates)
Group 3	Vegetation detection
Group 4	Broad absorptions in the 1.5-micron region
Group 5	Broad absorptions in the 2-micron region
Case 1	Vegetation red edge shift
Case 2	Vegetation spectral type
Case 3	Vegetation water band depth: 0.95-micron band
Case 4	Vegetation water band depth: 1.15-micron band
Case 5	Vegetation water band depth: 1.4-micron band

4.2.2 EMIT-10 Aggregation

The complete set of continuum-normalized band depths must be aggregated together to the relevant EMIT-10 minerals, defined formally as the set M = {calcite, chlorite, dolomite, goethite, gypsum, hematite, illite, kaolinite, montmorillonite, and vermiculite}. Two additional mineral categories, "other iron oxides," and "all other minerals," account for the remaining minerals not in the EMIT-10, and augment M to 12 categories in total. We aggregate to the 12 mineral categories by calculating

$$SA_m^i = \sum_{j \in J} s_m^j a_i^j \ , \tag{5}$$

where SA_m^i is the spectral abundance of mineral $m \in M$, J is the set of all library constituents, and s_m^j is the fractional abundance of mineral m in constituent j, which we assume here is equal to the weight fraction. In the USGS 06 spectral library, this value is specified directly for

mineral constituents of non-intimate mixtures. For intimate mixtures, the relative weight fractions are specified. This process is demonstrated at a high-level in Figure 3.

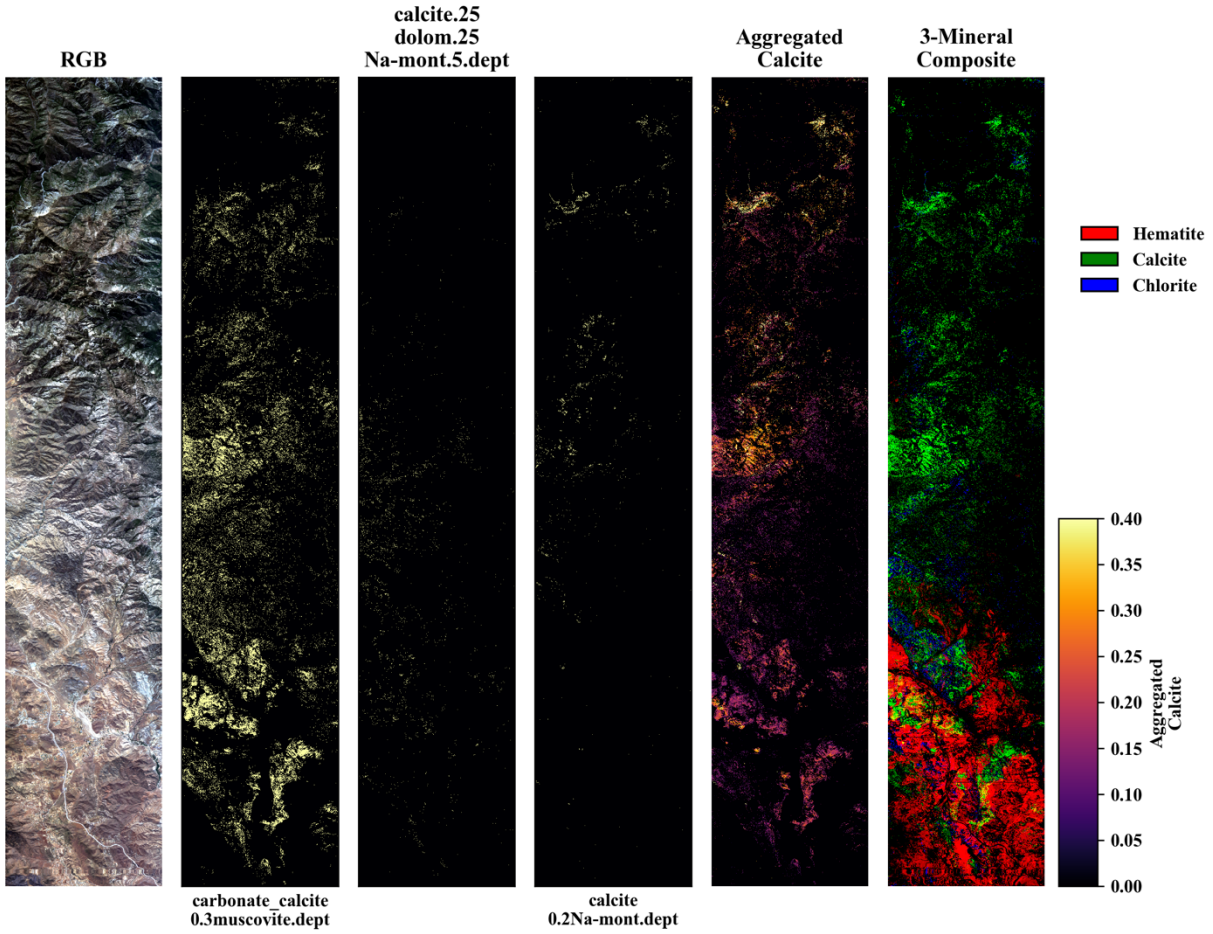

Figure 3. Demonstration of mineral aggregation to the core EMIT minerals. From the left, the diagram shows a 3-channel RGB sample slice of the reflectance data, followed by the three most prevalent calcite containing constituents within the reference library, displayed as binary presence-absence format for visual acuity. All calcite-containing minerals are then aggregated together to spectral abundances, as shown in the 5th panel. This is repeated for each EMIT mineral, as well as the two catch-all categories, as demonstrated through the 3-channel composite in the last panel.

4.3 Practical Considerations

Computation is largely input-output limited, and the calculations are fast relative to L2a. All relevant dependencies, including spectral reference libraries, are available on the official repository.

5. Output Data

Level 2b output data include both *delivered* products, which are necessary for mission success, as well as *auxiliary* products, which are generated in the process of producing the delivered products, and preserved for transparency and issue tracking.

4.4.1 Delivered Products

1. **Estimated mineral spectral abundance,** provided as *n* x 1280 x 12 BIL interleave data cubes, where each band corresponds to the one of the 10 identified EMIT mineral classes. Two additional bands account for "all other iron oxides," and "all other minerals" detected using the Tetracorder spectral reference library. Each channel contains the estimated mineral spectral abundance, as defined in Section 4.2.2.
2. **Estimated EMIT-10 mineral spectral abundance uncertainty,** provided as *n* x 1280 x 12 BIL interleave data cubes, where each channel corresponds to the one of the 10 identified EMIT mineral classes. Two additional channels account for "all other iron oxides," and "all other minerals" detected in the Tetracorder spectral reference library. Each channel contains the estimated EMIT mineral spectral abundance uncertainty, as defined in Section 5.

4.4.2 Auxiliary Products

1. **Normalized band depth,** provided as an *n* x 1280 x *c* BIL interleave data cube. Each channel contains the continuum and reference-library normalized band depth for each reference library constituent, as defined in section 4.2.2.
2. **Normalized band depth uncertainty,** provided as an *n* x 1280 x *c* BIL interleave data cube. Each channel contains the estimated uncertainty for the continuum and reference-library normalized band depth for each reference library constituent, as defined in section 5.

6. Calibration, uncertainty characterization and propagation, and validation

6.1 Uncertainty quantification

Uncertainty characterization of the L2b product is calculated by propagating wavelength-specific measurement uncertainty forward from the L2a product. For simplicity, we approximate the uncertainty of a continuum removed reflectance feature at a particular wavelength (e.g. $O_j^i(w)$) as the measurement uncertainty of the reflectance spectrum at that same wavelength, which we denote as $\Psi_R(w)$, relying on the assumption that the continuum endmember definitions build no additional uncertainty into the calculation. This allows us to directly calculate the uncertainty of a_j^i, denoted as $\Psi_{a_j}^i$, as

$$\Psi_{a_j}^i = \sqrt{\left(\frac{1}{\sum_{w\in W} L_j^2(w) - \left(\sum_{w\in W} L_j(w)\right)^2}\right)^2 \sum_{w\in W}\left(\left(nL_j(w) - \sum_{v\in W} L_j(v)\right)^2 {\Psi_R}^2(w)\right)} \quad (6)$$

where as above, SA_m^i is the spectral abundance of mineral $m \in M$ and L_j is the continuum-normalized reflectance of the library reference materials. As the calculation of SA_m^i is linear with respect to a_j^i, we can then carry forward this uncertainty term to our ultimate uncertainty estimation for each of the 12 mineral categories, $\Psi_{SA_m^i}$, by assuming the independence of each constituent uncertainty, giving

$$\Psi_{SA_m^i} = \sqrt{\sum_{j\in J} {s_m^j}^2 {\Psi_{a_j}^i}^2}\ . \quad (7)$$

While $\Psi_{SA_m^i}$ represents a reasonable estimation of the propagated surface reflectance uncertainty, several additional sources of potential error are not considered here. Most notably, this includes any misidentification of minerals within the spectral library, which would not be captured. With imaging spectroscopy measurements being taken for many regions of the planet for the first time, is possible that spectra of additional materials will need to be added to the reference library in order to better characterize materials that conflict with those that aggregate together to calculate *SA*. This is consistent with previous use of the Tetracorder system, though the need for augmentation of spectral libraries used in studies with Tetracorder have decreased over time. A significant round of spectral reference library augmentations were made circa 2010 to incorporate organics and man-made materials found in urban environments (Clark et al., 2010; Kramer et al., 2010; Pieters et al., 2010; Swayze et al., 2009), and since then newer studies have introduced significantly fewer changes (e.g. Swayze et al. (2014)), as compared to earlier studies.

6.2 Validation at Known Sites

The Tetracorder mineral identification approach has been previously validated at numerous desert sites throughout the Southwestern U.S. (Clark et al., 2003 and Swayze et al., 2014), based primarily on laboratory electron probe microanalysis, petrographic, SEM, spectroscopic, and X-ray diffraction measurements of samples collected from areas spectrally dominated by one or more VSWIR active minerals including those on the EMIT list.

Validation of EMIT specific Tetracorder products can be accomplished by comparison of EMIT L2b products with those equivalently derived from AVIRIS data. Relevant regions with extensive coverage that have been relatively well (mineralogically) characterized, and which have significant enough coverage so as to likely be included in EMIT coverage, include those shown in Table 3.

Table 3. EMIT mineral mapping validation sites and their minerals.

Mineral Validation Site	Spectrally Dominant Mineralogy
Arches National Park, Utah	Calcite, dolomite, goethite, gypsum, hematite, illite, kaolinite, montmorillonite
Cuprite, Nevada	Calcite, chlorite, goethite, hematite, illite, kaolinite, calcite, montmorillonite
Mountain Pass, California	Dolomite, vermiculite
Salton Sea area, California	Carbonates, goethite, hematite, kaolinite
White Sands, New Mexico	Gypsum

7. Constraints and Limitations

No constraints or limitations are imposed on the L2b products. All delivered data will have undergone quality control and should be considered valid, calibrated data up to the reported uncertainties in input parameters. Unanticipated data corruption due to factors outside the modeling, if discovered, will be reported in peer reviewed literature and/or addenda to this ATBD.

8. Code Repository and References

References

Clark, R. N., R. O. Green, G. A. Swayze, G. Meeker, S. Sutley, T. M. Hoefen, K. E. Livo, G. Plumlee, B. Pavri, C. Sarture, S. Wilson, P. Hageman, P. Lamothe, J. S. Vance, J. Boardman I. Brownfield, C. Gent, L. C. Morath, J. Taggart, P. M. Theodorakos, and M. Adams, 2001, Environmental Studies of the World Trade Center area after the September 11, 2001 attack. U. S. Geological Survey, *Open File Report OFR-01-0429*, (approximately 260 pages printed), 2001. http://pubs.usgs.gov/of/2001/ofr-01-0429/

Clark, R.N., Swayze, G.A., Livo, K.E., Kokaly, R.F., Sutley, S.J., Dalton, J.B., McDougal, R.R., and Gent, C.A. 2003. Imaging spectroscopy: Earth and planetary remote sensing with the USGS Tetracorder and expert systems, *Journal of Geophysical Research*, Vol. 108(E12), 5131, doi:10.1029/2002JE001847, p. 5-1 to 5-44.
http://speclab.cr.usgs.gov/PAPERS/tetracorder

Clark, R.N., G.A. Swayze, T.M. Hoefen, R.O. Green, K.E. Livo, G., Meeker, S. Sutley, G. Plumlee, B. Pavri, C. Sarture, J. Boardman, I., Brownfield, L.C. Morath, 2006, Chapter 4: Environmental mapping of the World Trade Center area with imaging spectroscopy after the September 11, 2001 attack: in *Urban Aerosols and Their Impacts: Lessons Learned from the World Trade Center Tragedy*, Jeff Gaffney and N. A. Marley (eds), *American Chemical Society*, Symposium Series 919, Oxford University Press, p. 66-83, plates 4.1-4.6.

http://www.us.oup.com/us/catalog/general/subject/Chemistry/EnvironmentalChemistry/?view=usa&ci=9780841239166

Clark, R.N., Swayze, G.A., Wise, R., Livo, E., Hoefen, T., Kokaly, R., Sutley, S.J., 2007, USGS digital spectral library splib06a: *U.S. Geological Survey Data Series 231*, http://speclab.cr.usgs.gov/spectral-lib.html with over 6000 web pages, and data files.

Clark, R.N., Swayze, G.A., Leifer, I. Livo, K.E., Kokaly, R., Hoefen, T., Lundeen, S., Eastwood, M., Green, R.O., Pearson, N., Sarture, C., McCubbin, I., Roberts, D., Bradley, E., Steele, D., Ryan, T., Dominguez, R., and the Air borne Visible/Infrared Imaging Spectrometer (AVIRIS) Team, 2010, A method for quantitative mapping of thick oil spills using imaging spectroscopy: *U.S. Geological Survey Open-File Report 20101167*, 51 p. http://pubs.usgs.gov/of/2010/1167/

Green, R.O., Eastwood, M.L., Sarture, C.M., Chrien, T.G., Aronsson, M., Chippendale, B.J., Faust, J.A., Pavri, B.E., Chovit, C.J., Solis, J., Olah, M.R., Williams, O., 1998, Imaging spectroscopy and the Airborne Visible/Infrared Imaging Spectrometer (AVIRIS): *Remote Sensing of Environment*, v. 65, p. 227-248.

Kokaly, R.F., R. N. Clark, G. A. Swayze, K. E. Livo, T. M. Hoefen, N. C. Pearson, R. A. Wise, W. M. Benzel, H. A. Lowers, R. L. Driscoll, and A. J. Klein, 2017, USGS Spectral Library Version 7: U.S. Geological Survey Data Series 1035, 61 p., https://doi.org/10.3133/ds1035. https://speclab.cr.usgs.gov/spectral-lib.html

Kramer, Georgiana Y., Sebastien Besse, Jeffrey Nettles, Jean-Philippe Combe, Roger N. Clark, Carle M. Pieters, Matthew Staid, Erik Malaret, Joseph Boardman, Robert O. Green, Thomas B. McCord, James W. Head III, 2010, Newer Views of the Moon: Comparing Spectra from 1 Clementine and the Moon Mineralogy Mapper, *J. of Geophysical Research* **116**, E00G04, doi:10.1029/2010JE003728.

Li, L., Mahowald, N., Balkanski, Y., Connelly, D., Ginoux, P., Ageitos, M. G., Hamilton, D., Kalashnikova, O., Klose, M., Miller, R. L., Obiso, V., Paynter, D. and Perez Garcia-Pando, C.: Large contribution of hematite and geothite to uncertainty in dust direct radiative forcing, Atmos. Chem. Phys., 2020.

Livo, K.E., Kruse, F.A., Clark, R.N., Kokaly, R.F., and Shanks, W.C. III, 2007, Hydrothermally Altered Rock and Hot- Spring Deposits at Yellowstone National Park—Characterized Using Airborne Visible- and Infrared-Spectroscopy Data, Chapter O in: Integrated Geoscience Studies in the Greater Yellowstone Area—Volcanic, Tectonic, and Hydrothermal Processes in the Yellowstone Geoecosystem, *USGS Professional Paper 1717*, 463-489.

Pieters, C. M., J. N. Goswami, R. N. Clark, M. Annadurai, J. Boardman, B. Buratti, J.-P. Combe, M. D. Dyar, R. Green, J. W. Head, C. Hibbitts, M. Hicks, P. Isaacson, R. Klima, G. Kramer, S. Kumar, E. Livo, S. Lundeen, E. Malaret, T. McCord, J. Mustard, J. Nettles, N. Petro, C. Runyon, M. Staid, J. Sunshine, L. A. Taylor, S. Tompkins, P. Varanasi, 2009, Character and Spatial Distribution of OH/H_2O on the Surface of the Moon seen by M3 on Chandrayaan-1 *Science*, **326**, 568-572, DOI: 10.1126/science.1178658.

Swayze, G. A., 1997, The hydrothermal and structural history of the Cuprite mining district, southwestern Nevada: An integrated geological and geophysical approach, Ph.D. thesis, 399 pp., Univ. of Colorado, Boulder, Colo.

Swayze, G.A., K.S. Smith, R.N. Clark, S.J. Sutley, R.N. Pearson, G.S. Rust, J.S. Vance, P.L. Hageman, P.H. Briggs, A.L. Meier, M.J. Singleton, and S. Roth, 2000, Using imaging spectroscopy to map acidic mine waste, *Environmental Science and Technology*, **34**. 47-54.

Swayze, G.A., Kokaly, R.F., Higgins, C.T., Clinkenbeard, J.P., Clark, R.N., Lowers, H.A., and Sutley, S.J., 2009, Mapping potentially asbestos-bearing rocks using imaging spectroscopy: *Geology*, **37**, 763-766.

Swayze, G.A., Clark, R.N., Goetz, F.H., Chrien, T.G., and Gorelick, N.S., 2003, Effects of spectrometer band pass, sampling, and signal-to-noise ratio on spectral identification using the Tetracorder algorithm: *Journal of Geophysical Research* (Planets), **108**, 5105, doi: 10.1029/2002JE001975, 30 p.

Swayze, G.A., Clark, R.N., Goetz, A.F.H, Livo, K.E., Breit, G.N., Sutley, S.J., Kruse, F.A., Snee, L.W., Lowers, H.A., Post, J.L., Stoffregen, R.E., and Ashley, R.P., 2014, Mapping advanced argillic alteration at Cuprite, Nevada using imaging spectroscopy: *Economic Geology*, **109**, 1179-1221 DOI: 10.2113/econgeo.109.5.1179